Published in final edited form as:

J Comput Chem. 2018 July 15; 39(19): 1259–1266. doi:10.1002/jcc.25190.

Semiempirical Configuration Interaction Calculations for Ru-Centered Dyes†

Lisa A. Fredin,

Thomas C. Allison

Chemical Informatics Research Group, Chemical Science Division, Material Measurement Laboratory, National Institute of Standards and Technology, 100 Bureau Drive, Stop 8320, Gaithersburg, Maryland 20899-8320

Abstract

Computational investigation of the photochemical properties of transition-metal-centered dyes typically involves optimization of the molecular structure followed by calculation of the UV/visible spectrum. At present, these steps are usually carried out using density functional theory (DFT) and time-dependent DFT calculations. Recently, we demonstrated that semiempirical methods with appropriate parameterization could yield geometries that were in very good agreement with DFT calculations, allowing large sets of molecules to be screened quickly and efficiently. In this article, we modify a configuration interaction (CI) method based on a semiempirical PM6 Hamiltonian to determine the UV/visible absorption spectra of Ru-centered complexes. Our modification to the CI method is based on a scaling of the two-center, two-electron Coulomb integrals. This modified, PM6-based method shows a significantly better match to the experimental absorption spectra versus the default configuration interaction method (in MOPAC) on a training set of 13 molecules. In particular, the modified PM6 method blue-shifts the location of the metal-to-ligand charge-transfer (MLCT) peaks, in better agreement with experimental and DFT-based computational results, correcting a significant deficiency of the unmodified method. Published 2018. This article is a U.S. Government work and is in the public domain in the USA

Keywords

semiempirical methods; PM6; configuration interaction; UV/visible

Introduction

Traditional semiempirical calculations of UV/visible spectra of transition-metal-centered complexes provide unphysical results; however, scaling the PM6 two-center, two-electron Coulomb integrals significantly improves the match to experimental absorption spectra, making the methodology well-suited for rapid computational screening of light-harvesting

lisa.fredin@nist.gov .

Additional Supporting Information may be found in the online version of this article.

dye molecules. These molecules take sunlight and convert it to energy or electrons that can then be used in photovoltaic[1–10] or photocatalytic[11–14] applications. Molecular dyes have been under particularly deep investigation due to their stability and well-defined chemistry. The usefulness of these dyes depends on the overlap of the dye absorption bands with the white light spectra, the energetics of the dye excited states, and the efficiency of the production of electrons.

Organic dyes,[2–4] transition metal-centered complexes, and Zn-porphyrins[1,15,16] have been developed for a variety of applications. Metal-centered dye complexes, such as Ru(II)-containing compounds,[17–22] analogues based on Fe(II),[23,24] Cu(I),[25] and other earth abundant metals,[26] as well as metal porphyrins, provide high dye-sensitized solar cell (DSC) efficiencies due to their highly favorable excited state properties.[27–32] Ru(II)-polypyridyl complexes have led to some of the highest measured DSC efficiencies to date[33] due to the alignment of their excited states with the titania conduction band and favorable redox properties.[19,34,35] Nevertheless, the cost of molecular light harvesting per unit energy output remains too high to make them competitive with their silicon-based counterparts.

In metal-centered complexes, ligand field theory states that the coordination geometry and electron density on the metal center control the redox and excited state properties. The lowest-energy excitations in these dyes are typically metal-to-ligand charge transfer (MLCT) states where electrons from the highest occupied molecular orbitals (HOMOs), e.g. Ru(II)-t_{2g}, are excited into low-lying ligand lowest unoccupied molecular orbitals (LUMOs). The predicted energies of such transitions are directly related to the coordination geometry, types of ligands, and metal–ligand binding, all of which can be predicted using quantum chemistry. In the hunt for chromophores with higher efficiency, computational methods can provide predictive structures and ultraviolet–visible (UV/vis) spectra that can be used to screen for promising new chromophores.

Computational screening has been a powerful means to new scientific insight and discovery for applications from drug to materials design.[36–39] By examining a large number of structures, it is possible to optimize for desirable properties and to explore structures that one might not otherwise consider. The drawback to this approach is that it may require a significant amount of time and resources if the computational method is relatively expensive. The molecules considered in this article, Ru-based light harvesting chromophores, are typically investigated using density functional theory (DFT), involving optimization of the molecular structure followed by calculation of the UV/vis spectrum (time-dependent DFT). While this process is relatively cost effective for a few compounds at a time, it is prohibitively time consuming for large scale screening applications (e.g., thousands of compounds).

To realize a complete screening methodology for transition metal dyes, it is necessary to be able to optimize candidate molecular structures and compute their UV/vis spectrum quickly, cheaply, and accurately. In a previous publication,[40] we showed that geometries calculated using Ru basis set parameters optimized for the semiempirical PM6 Hamiltonian[41] for Ru-centered dye-sensitized solar cell molecules were in good agreement with optimized DFT geometries. As mentioned in that article, the speed and accuracy of the PM6 method,

particularly with optimized basis set parameters, makes it an excellent candidate for computational screening of the geometries of thousands of candidate dyes.

There is a long history of using semiempirical methods to compute UV/vis spectra. Some of the earliest calculations were made using the Pariser–Parr–Pople scheme.[42,43] Finding that this method was not suitable for studying $\pi \rightarrow \pi^*$ transitions, Del Bene and Jaffé[44] modified a complete neglect of differential overlap (CNDO) method to compute UV/vis spectra for an isoelectronic series of benzene derivatives. In that article, which was the first in a series of articles on small molecule UV/vis spectroscopy, good results for $n \rightarrow \pi^*$ and $\pi \rightarrow \pi^*$ singlet–singlet transitions were obtained. A few years later, Ridley and Zerner introduced a method based on the intermediate neglect of differential overlap (INDO) method of Pople and coworkers[45–48] and used it to study pyrrole and azine compounds. In a subsequent article, the same authors examined triplet states of benzene, pyridine, and diazine compounds.[49] Zerner and coworkers later extended their model to the study of transition metal complexes, using an INDO-based method to compute the UV/vis spectrum of ferrocene.[50] More recently, Klamt implemented a method for calculating UV/vis spectra of solvated molecules[51] into the MOPAC* package[52] based on the modified neglect of diatomic overlap (MNDO) method of Dewar and Thiel.[53] However, in this article, Klamt did not make substantial comparisons to experimental data “due to the well-known deficiencies of the MNDO Hamiltonian available in MOPAC in the calculation of electronic excitation spectra.”[51]

Early efforts to compute UV/vis spectra focused primarily on modifications to the Coulomb integrals, and considerable effort was devoted to developing new parameters for use in the semiempirical method.[50,54] Modern semiempirical methods such as PM6[41] and PM7[55] have parameter sets that have been extensively optimized based on data that was not available in parameterizing the CNDO and INDO methods of earlier works, significantly increasing their accuracy. Furthermore, these methods use an spd basis instead of the simpler sp basis of the earlier work, making them more appropriate for calculations involving transition metals.

In this article, we optimize parameters for a new Ru basis set for structure optimization using PM6 as implemented in MOPAC and modify the Coulomb integrals for the configuration interaction (CI) calculation of the UV/vis spectrum to improve agreement with experimental absorption maxima. The UV/vis spectra of a training set of 13 molecules computed using the modified PM6 CI show improved accuracy compared to the unmodified PM6 CI, reducing the mean unsigned error from 67.3 nm to 29.7 nm. This improved, semiempirical CI method provides the opportunity to screen thousands of light harvesting dyes.

*Certain commercial equipment, instruments or materials are identified in this paper to specify the experimental procedure adequately. Such identification is not intended to imply recommendation or endorsement by the National Institute of Standards and Technology, nor is it intended to imply that the materials or equipment identified are necessarily the best available for the purpose.

Methodology

A set of 13 test compounds, spanning representative Ru-complex and Ru-bonding types, was created for use in parameterizing the UV/vis spectroscopic CI method[51] implemented in MOPAC.[52] The largest group of Ru(II) dyes in the test set uses polypyridyl ligands that bind to the Ru center via Ru–N bonds, and the two major polypyridyl motifs are tris-bidentate and bis-tridentate complexes. Thus, homoleptic bidentate $Ru(BPy)_3$,[56] tridentate *meridional* $Ru(TPy)_2$,[57] and N3 (*cis–bis*(isothiocyanato) *bis*(2,2″-bipyridyl-4,4″-dicarboxylato ruthenium(II))[17,58] and its tridentate derivative black-dye[59] (*tris*-thiocyanato-2,2′:6′,2″-terpyridine-4,4′,4″-tricarboxylato ruthenium(II)) are included. In addition, various ligand binding groups in tridentate ligands are included via $Ru(DQP)_2$[18] (DQP = 2,6-di(8-quinolin-8-yl)-pyridine), and its 4-substituted analogs $Ru(DQPCOOH)_2$,[60] $Ru(DQPNH_2)_2$,[60] $Ru(PzPyPz)_2$ (PzPyPz = 2,6-di(pyrazol-1-yl) pyridine, sometimes called bpp),[61] $Ru(DBPzP)_2$ (DBPzP = 2,6-dibenzopyrazolyl-pyridine),[62] $Ru(DCpP)_2$ (DCpP = 6-*bis*(2-carboxypyridyl) pyridine),[63] $Ru(DNinP)_2$ (DNinP = 2,6-di(*N*-7-azaindol-1-yl) pyridine),[22] $Ru(DQxP)_2$ (DQxP = 2,6-di(quinoxalin-5-yl) pyridine),[22] and $Ru(DQPz)_2$ (DQPz = 1,3-*bis*(8-quinolinyl) pyrazole).[20] This extensive set of complexes gives a broad representation of ligands incorporating Ru–N bonding and are listed by abbreviated names and formulas in Table 1.

To optimize the Ru basis set for Ru-DSC geometries, a testing set of 20 molecules that contains the 13 molecules listed above and identical to the set used in our previous paper,[40] was used. From this set, a training set of 5 molecules ($Ru(DQPl)_2$ (DQPl = 1,3-*bis*(8-quinolinyl)-pyrrole), $Ru(DQPNH_2)_2$, $Ru(DQP)_2$, $Ru(DQPzP)_2$, $Ru(TPy)_2$) was taken. This training set differs from the one used in our previous paper.[40] (Optimized geometries of all 20 molecules are given in the Supporting Information.) Using the methodology described in our previous article,[40] we have optimized a Ru basis set for PM6 as implemented in MOPAC (Tables 2 and 3). Differences in the training set and parameters exposed in the MOPAC implementation of PM6 led to the need for a new optimization of the basis set. Again, it was found that it was sufficient to optimize the basis set for Ru alone to improve the agreement between the PM6 and the DFT structures. When this optimized Ru basis set (rRu) is used, the mean unsigned error in Ru–ligand bond lengths is reduced from 0.041 Å to 0.022 Å for the testing set, and the mean unsigned error in Ru–ligand bond angles is reduced from 0.85° to 0.78°. As was found previously,[40] though the magnitude of these differences is small, the effect on the calculated TDDFT UV/vis spectra is significant, justifying the use of the modified basis set.

To find a suitable method for computing UV/vis spectra using the PM6 semiempirical Hamiltonian, we proceed in a similar manner to that used to optimize the Ru basis set by assuming that the PM6 Hamiltonian provides a good general description of Ru-centered dyes, and that it can be improved by suitable parameterization. Taking inspiration from previous work to develop improved semiempirical methods for UV/vis spectra, we examined modifications of the Coulomb integral parameters.

In previous work, considerable effort was devoted to deriving improved values for the Coulomb integral parameters and to modifying the functional form of two-center, two-

electron Coulomb integrals to incorporate distance dependence via the Mataga–Nishimoto function.[64] These strategies and others were investigated as part of this work, but were found to be less accurate than the method ultimately employed. This is attributed, at least in part, to the care that went into the derivation of the PM6 parameters and to the considerably more accurate experimental data that is available compared to that available in the 1960s when the first models were being built and tested. In particular, data on atomic energy levels yields qualitatively different conclusions than that available to Zerner and coworkers[50] in their work.

Thus, it was found that the default Coulomb integral parameters of the PM6 method were quite accurate, and that no further modification of these parameters was justified. Instead, to produce more accurate UV/vis spectra within the PM6 method, the two-center, two-electron Coulomb integrals were scaled. The two-center, two-electron Coulomb integrals of the PM6 method as implemented in the MOPAC semiempirical quantum chemistry code[52] are modified using six multiplicative scaling factors f_{ss}, f_{sp}, f_{sd}, f_{pp}, f_{pd} and f_{dd} that are applied to the corresponding spd Coulomb integral (J), e.g. $J'_{sp} = f_{sp}J_{sp}$. These scaling factors were implemented into the MOPAC code[52] by modifying the wrtkey subroutine to read scaling factor values from the MOPAC input file and the mndod sub-routine where the scaling was applied to the Coulomb integrals.

The values of these scaling factors were optimized using the Powell method[65] as implemented in the SciPy computational library.[66] The Powell method has the advantage that it does not require derivatives of the optimization function and has proven to be efficient and reliable in previous work. The optimization used a root mean squared error function

$$\varepsilon = \sqrt{\frac{1}{N}\sum_{i=1}^{N}\left(E_{\mathrm{calc},i} - E_{\mathrm{expt}}\right)^2} \tag{1}$$

where E_{calc} and E_{expt} are the computed and experimental values of the UV/vis spectral lines. The sum in the equation above was restricted to singlet–singlet transitions in the range of 1.7 eV–4.2 eV, corresponding to the spectral region of interest for screening light-harvesting performance. Absorption energies were calculated within MOPAC using all single and double excitations within an active space of five molecular orbitals, including two doubly occupied orbitals, as implemented in the multi-electron configuration interaction (MECI) module of the code. (Active spaces of different sizes were investigated, as reported in the SI, and the spectra did not differ substantially from the spectra calculated using the (5,2) active space.) The difference between the calculated and experimental values in the error term was evaluated using the experimental value closest to the calculated value, i.e.

$$\left|E_{\mathrm{calc},i} - E_{\mathrm{expt}}\right| = \min_j \left|E_{\mathrm{calc},i} - E_{\mathrm{expt},j}\right| \tag{2}$$

All fitting was performed with energies in units of eV. There was no requirement for all experimental absorption lines to be matched in the optimization procedure, no penalty was imposed during optimization if the number of calculated lines was less than (or greater than) the number of experimental lines, and the magnitude of the intensity was not considered (however, transitions with intensity less than 0.01 were not included). In cases where the CI calculation did not yield any singlet transitions in the appropriate range for a particular compound, a large value was used in the error summation, and the optimization was allowed to proceed. During the fitting process, the parameters were constrained to values in the range of 1±0:05 as previous experience dictated that small scalings of the Coulomb integrals were sufficient to produce good results. Optimizer steps that exceeded these bounds were rejected by assigning them a large error value. The optimization typically proceeded until no further improvement in the objective function was able to be achieved. To reduce the possibility that the optimized parameters represent a local minimum and to find the best set of scaling factors, the optimization was run many times starting from different, randomly generated initial guesses for the parameters and with different bounds on the parameter values. This by no means indicates that the global minimum parameter set has been found.

Results

The optimized Coulomb integral scaling parameters obtained in this manner are presented in Table 4 and the fitting set of spectral lines is given in Table 5. The data given in the latter and subsequent tables as well as figures are in units of nm, a unit more commonly used than eV when plotting UV/vis spectra. It is interesting to note that the scaling parameters in Table 4 show that optimizing the performance of the CI calculation for UV/vis spectra requires changes in the values of the Coulomb integrals of about 1%.

Statistical data calculated for the default configuration interaction (PM6CI) with the default basis set (Fig. 1) and with the optimized Ru basis set (rRu, Fig. 2), as well as the scaled Coulomb CI (PM6scCI) with the optimized Ru basis set (Fig. 3) are shown in Table 6. In our previous paper,[40] it was shown that accurate geometries were important for reproducing calculated transitions. From this table it is clear that use of the optimized Ru basis set is not sufficient by itself to improve the UV/vis results calculated using PM6. The use of the scaled Coulomb CI with the optimized geometries is effective in reducing the error measures, providing the best match to the experimental data. In general, the spectra contain only metal-to-ligand excitations, an indication that the MLCT region is being captured adequately by the model in the range of 350–700 nm.

This can be seen even more clearly by directly comparing the three sets of computed transitions to the experimental data. It is immediately evident that PM6 with the default basis set and no scaling of the Coulomb integrals (Fig. 4) produces transitions that for the most part lie toward the right side of the plot (lower energy) compared to the experimental values. This is an indication of the inadequate performance of the unoptimized/unscaled approach.

The second comparison, calculated using the optimized Ru basis set (rRu), but without using scaled Coulomb integrals in the CI calculations, is a direct measure of the improved geometries on the PM6 UV/vis calculation. The effect of the optimized geometry is dramatic

and immediately evident (Fig. 5). This correlates well with the results we saw previously where an optimized Ru basis set improved the time-dependent DFT (TDDFT) spectra.[40] The positions of the maxima are shifted to higher energies and show better agreement with the experimental data. However, there are several spectra in which there are either no absorption energies in the plotted range (e.g., $Ru(BPy)_3$) or where the disagreement is particularly bad (e.g., $Ru(DCpP)_2$). Also, several plots show unphysical behavior (e.g., Ru black-dye and $Ru(TPy)_2$) with substantial peaks extending into the 600–700 nm region.

Finally, the results of the CI calculation performed using the scaled Coulomb integrals with geometries optimized using the optimized Ru basis set (Fig. 6) clearly demonstrate that the optimized CI method has removed the spurious tails present in the previous plot and maintained the improved performance of the location of the peak maxima. It is evident from the stick spectra plot that the agreement is not perfect, but it is generally improved and the experimental trends are preserved. Since small changes in geometric structure shift the calculated transitions, we tried to obtain UV/vis spectra that more closely matched the experimental lineshapes by Boltzmann weighting the spectra calculated along the ligand–Ru breathing mode (details in the SI). While the calculated transitions at each geometry along the breathing mode (Supporting Information Fig. S1) are shifted relative to the optimized minimum, the energetics are such that the probability of these non-equilibrium modes is so small that the Boltzmann weighted spectrum (Supporting Information Fig. S2) is dominated by the optimized structure. Thus, the use of the Boltzmann weighting procedure was found to offer no advantage over the single spectrum calculation.

Discussion

To demonstrate the performance of our method, we show three representative cases in Figure 7 comparing semiempirical UV/vis spectra to TDDFT and the experimental maxima. For cases where the error of our method is large compared to experiment and TDDFT, like Ru-N3, our optimized method qualitatively captures the MLCT peaks, and is a clear improvement over the default CI. For $Ru(DQPzP)_2$, the PM6scCI spectra has moderate error when compared to the experimental spectrum, and does not exhibit the unphysical tail present in the TDDFT results. In addition, this is a rare case where the PM6CI predicts a high-energy maximum transition, indicating that our PM6scCI method is successfully optimizing toward experiment regardless of whether the base method is higher or lower in energy. Finally, the PM6scCI spectrum of $Ru(PzPyPz)_2$ is in excellent agreement in the MLCT region with experiment and TDDFT, showing a significant improvement over the PM6CI result.

Overall, optimization of the Coulomb integral scaling factors reduced the fitting error (vs. the results produced with no scaling of the Coulomb integrals) of the PM6CI prediction of UV/vis spectra for the 13 test compounds by more than a factor of eight, with a final root mean squared fitting error [eq. (1)] of the calculated results from the experimental spectral lines of 0.23 eV. CI calculations using unscaled Coulomb integrals on the same compounds at the same geometries yielded a root mean squared fitting error [eq. (1)] of 1.94 eV. This degree of deviation and the unphysical nature of the default CI (PM6CI) predicted spectra

(the transitions are too low in energy, Fig. 2) justifies the concerns about the use of various MNDO-based methods for the calculation of UV/vis spectra.

Examining the results presented in Table 5 more closely, it is clear that the error is dominated by a few molecules such as $Ru(DNinP)_2$, $Ru(DQPz)_2$, and N3. For most molecules, the deviation is much more modest. This suggests that some improvement in parameterization, methodology, or optimized geometry will be required to reduce the error further for these three compounds, or perhaps that the limits of the semiempirical approach (e.g., minimal basis set, neglect of certain integrals) are being reached. It is also possible that more rigorous fitting of the DFT absorption energies and intensities will yield better results. However, we have chosen comparison with experiment as a more rigorous test of the methodology. The parameters presented in this article are thus sufficient to produce UV/vis for screening applications.

The speed with which the configuration interaction calculation may be carried out in MOPAC, combined with the improved accuracy afforded by the present improved PM6 method, makes it well suited for screening applications. In testing, rates of more than 500 molecules per hour were achieved on a modest desktop computer, making it is possible to examine a large number of candidate molecules in a single day. For reference, calculating $Ru(BPy)_2$ UV/vis excitations on the same computer takes 0.25 s using PM6scCI in MOPAC as compared to >550,000 s for the same number of TDDFT transitions (55 for $Ru(BPy)_2$) in Orca.[67,68] Thus, the method presented here provides a way to calculate the absorption spectra of Ru-centered dyes that is approximately 6 orders of magnitude faster than traditional TDDFT, and provides the first accurate and fast semi-empirical screening procedure for Ru complexes. For any candidates of particular interest, further higher-level DFT calculations can be used to verify the results of the semiempirical model. Using the semiempirical model in this way will drastically reduce the time required to scan a large chemical space for candidate light harvesting dyes, allowing the best candidates to proceed to more rigorous testing.

Conclusions

In this article, UV/vis spectra have been computed using a modified version of the PM6 semiempirical Hamiltonian. The essence of the method is the optimization of molecular geometries using an optimized basis set for Ru and a configuration interaction calculation in which the two-center, two-electron Coulomb integrals are scaled. Optimization of the scaling parameters yields a significant improvement in the predicted UV/vis spectra. The resulting method shows good agreement with experimental data and with time-dependent density functional theory calculations, indicating its predictive value for screening large sets of candidate dye molecules.

Supplementary Material

Refer to Web version on PubMed Central for supplementary material.

References

[1]. Mathew S, Yella A, Gao P, Humphry-Baker R, Curchod BFE, Ashari-Astani N, Tavernelli I, Rothlisberger U, Nazeeruddin MK, Grätzel M, Nat. Chem 2014, 6, 242. [PubMed: 24557140]

[2]. Hagberg DP, Edvinsson T, Marinado T, Boschloo G, Hagfeldt A, Sun L, Chem. Commun 2006, 0, 2245.

[3]. Hagberg DP, Yum J-H, Lee H, De Angelis F, Marinado T, Karlsson KM, Humphry-Baker R, Sun L, Hagfeldt A, Grätzel M, Nazeeruddin MK, J. Am. Chem. Soc 2008, 130, 6259. [PubMed: 18419124]

[4]. Kusters J, Feldt SM, Gibson E. a., Gabrielsson E, Sun L, Boschloo G, Hagfeldt A, Kusters J, J. Am. Chem. Soc 2007, 1, 2.

[5]. Kamat PV, J. Phys. Chem. Lett 2013, 4, 908. [PubMed: 26291355]

[6]. Kojima A, Teshima K, Shirai Y, Miyasaka T, J. Am. Chem. Soc 2009, 131, 6050. [PubMed: 19366264]

[7]. Kim H-S, Lee C-R, Im J-H, Lee K-B, Moehl T, Marchioro A, Moon S-J, Humphry-Baker R, Yum J-H, Moser JE, Grätzel M, Park N-G, Sci. Rep. UK 2012, 2, 591.

[8]. Lee MM, Teuscher J, Miyasaka T, Murakami TN, Snaith HJ, Science 2012, 338, 643. [PubMed: 23042296]

[9]. Shoaee S, Clarke TM, Eng MP, McCulloch I, Durrant JR, Huang C, Barlow S, Marder SR, Espildora E, Delgado JL, Martin N, Campa BJ, Vanderzande D, Heeney MJ, Photon J. Energy 2012, 2, 021001.

[10]. Ohkita H, Ito S, Polymer 2011, 52, 4397.

[11]. Nocera DG, Acc. Chem. Res 2012, 45, 767. [PubMed: 22475039]

[12]. Nocera DG, Acc. Chem. Res 2017, 50, 616. [PubMed: 28945407]

[13]. Hammes-Schiffer S, Stuchebrukhov AA, Chem. Rev 2010, 110, 6939. [PubMed: 21049940]

[14]. Young KJ, Martini LA, Milot RL, Snoeberger RC, Batista VS, Schmuttenmaer CA, Crabtree RH, Brudvig GW, Coord. Chem. Rev2012, 256, 2503. [PubMed: 25364029]

[15]. Imahori H, Umeyama T, Ito S, Acc. Chem. Res 2009, 42, 1809. [PubMed: 19408942]

[16]. Li L-L, Diau EW-G, Chem. Soc. Rev 2013, 42, 291. [PubMed: 23023240]

[17]. Nazeeruddin MK, Kay A, Rodicio I, Humphry-Baker R, Mueller E, Liska P, Vlachopoulos N, Graetzel M, J. Am. Chem. Soc 1993, 115, 6382.

[18]. Abrahamsson M, Jäger M, Österman T, Eriksson L, Persson P, Becker H-C, Johansson O, Hammarström L, J. Am. Chem. Soc 2006, 128, 12616. [PubMed: 17002333]

[19]. Calvert JM, Caspar JV, Binstead RA, Westmoreland TD, Meyer TJ, J. Am. Chem. Soc 1982, 104, 6620.

[20]. Jarenmark M, Carlström G, Fredin LA, Wallenstein JH, Doverbratt I, Abrahamsson M, Persson P, Inorg. Chem 2016, 55, 3015. [PubMed: 26962970]

[21]. Abrahamsson M, Becker HC, Hammarström L, Bonnefous C, Chamchoumis C, Thummel RP, Inorg. Chem 2007, 46, 10354. [PubMed: 17975915]

[22]. Parada GA, Fredin LA, Santoni MP, Jäger M, Lomoth R, Hammarström L, Johansson O, Persson P, Ott S, Inorg. Chem 2013, 52, 5128. [PubMed: 23597274]

[23]. Liu Y, Persson P, Sundström V, Wärnmark K, Acc. Chem. Res 2016, 49, 1477. [PubMed: 27455191]

[24]. Abrahamsson M, In Photochemistry: Volume 44, Vol. 44, Chapter 7; Albini A, Fasani E, Eds.; The Royal Society of Chemistry: London, United Kingdom 2017, pp. 285–295.

[25]. Housecroft CE, Constable EC, Chem. Soc. Rev 2015, 44, 8386. [PubMed: 26356386]

[26]. Bozic-Weber B, Constable EC, Housecroft CE, Coord. Chem. Rev 2013, 257, 3089.

[27]. Gust D, Moore TA, Moore AL, Acc. Chem. Res 2009, 42, 1890. [PubMed: 19902921]

[28]. Sauvage JP, Collin JP, Chambron JC, Guillerez S, Coudret C, Balzani V, Barigelletti F, De Cola L, Flamigni L, Chem. Rev 1994, 94, 993.

[29]. Friedman AE, Chambron JC, Sauvage JP, Turro NJ, Barton JK, J. Am. Chem. Soc 1990, 112, 4960.

[30]. Ardo S, Meyer GJ, Chem. Soc. Rev 2009, 38, 115. [PubMed: 19088971]

[31]. Barigelletti F, Flamigni L, Chem. Soc. Rev 2000, 29, 1.

[32]. Alstrum-Acevedo JH, Brennaman MK, Meyer TJ, Inorg. Chem 2005, 44, 6802. [PubMed: 16180838]

[33]. Bignozzi CA, Argazzi R, Boaretto R, Busatto E, Carli S, Ronconi F, Caramori S, Coord. Chem. Rev 2013, 257, 1472.

[34]. Juris A, Balzani V, Barigelletti F, Campagna S, Belser P, von Zelewsky A, Coord. Chem. Rev 1988, 84, 85.

[35]. Winkler JR, Netzel TL, Creutz C, Sutin N, J. Am. Chem. Soc 1987, 109, 2381.

[36]. Mueller T, Kusne AG, Ramprasad R, Rev. Comp. Chem 2016, 29, 186.

[37]. Katsila T, Spyroulias GA, Patrinos GP, Matsoukas M-T, Comput. Struct. Biotechnol. J 2016, 14, 177. [PubMed: 27293534]

[38]. Emery AA, Saal JE, Kirklin S, Hegde VI, Wolverton C, Chem. Mater 2016, 28, 5621.

[39]. Sliwoski G, Kothiwale S, Meiler J, Lowe EWE, Pharmacol. Rev 2014, 66, 334. [PubMed: 24381236]

[40]. Fredin LA, Allison TC, J. Phys. Chem. A 2016, 120, 2135. [PubMed: 26982657]

[41]. Stewart JJP, J. Mol. Model 2007, 13, 1173. [PubMed: 17828561]

[42]. Pople JA, Trans. Faraday Soc. 1953, 49, 1375.

[43]. Pariser R, Parr RG, J. Chem. Phys 1953, 21, 466.

[44]. Del Bene J, Jaffé HH, J. Chem. Phys 1968, 48, 1807.

[45]. Pople JA, Santry DP, Segal GA, J. Chem. Phys 1965, 43, S129.

[46]. Pople JA, Segal GA, J. Chem. Phys 1965, 43, S136.

[47]. Pople JA, Segal GA, J. Chem. Phys 1966, 44, 3289.

[48]. Pople JA, Beveridge DL, Dobosh PA, J. Chem. Phys 1967, 47, 2026.

[49]. Ridley JE, Zerner MC, Theoret. Chim. Acta (Berl.) 1976, 42, 223.

[50]. Zerner MC, Loew GH, Kirchner RF, Mueller-Westerhoff UT, J. Am. Chem. Soc 1980, 102, 589.

[51]. Klamt A, J. Phys. Chem 1996, 100, 3349.

[52]. Stewart JJP, MOPAC2016, Stewart Computational Chemistry; Colorado Springs: Colorado Springs, CO 2016, http://OpenMOPAC.net (accessed 2017–09-20).

[53]. Dewar MJS, Thiel W, J. Am. Chem. Soc 1977, 99, 4899.

[54]. Ridley J, Zerner M, Theoret. Chim. Acta (Berl.) 1973, 32, 111.

[55]. Stewart JJP, J. Mol. Model 2013, 19, 1. [PubMed: 23187683]

[56]. Rillema DP, Jones DS, Woods C, Levy HA, Inorg. Chem 1992, 31, 2935.

[57]. Pyo S, Pérez-Cordero E, Bott SG, Echegoyen L, Inorg. Chem 1999, 38, 3337. [PubMed: 11671069]

[58]. Eskelinen E, Luukkanen S, Haukka M, Ahlgren M, Pakkanen TA, J. Chem. Soc. Dalton Trans. 2000, 0, 2745.

[59]. Péchy P, Renouard T, Zakeeruddin SM, Humphry-Baker R, Comte P, Liska P, Cevey L, Costa E, Shklover V, Spiccia L, Deacon GB, Bignozzi CA, Grätzel M, J. Am. Chem. Soc 2001, 123, 1613. [PubMed: 11456760]

[60]. Abrahamsson M, Jäger M, Kumar RJ, Österman T, Persson P, Becker H-C, Johansson O, Hammarström L, J. Am. Chem. Soc 2008, 130, 15533. [PubMed: 19006410]

[61]. Jameson DL, Blaho JK, Kruger KT, Goldsby KA, Inorg. Chem 1989, 28, 4312.

[62]. Bhaumik C, Das S, Saha D, Dutta S, Baitalik S, Inorg. Chem 2010, 49, 5049. [PubMed: 20469925]

[63]. Schramm F, Meded V, Fliegl H, Fink K, Fuhr O, Qu Z, Klopper W, Finn S, Keyes TE, Ruben M, Inorg. Chem 2009, 48, 5677. [PubMed: 19507851]

[64]. Mataga N, Nishimoto K, Z. Phys. Chem. Neue Folge 1957, 13, 140.

[65]. Powell MJD, Comput. J 1964, 7, 155.

[66]. Jones E, Oliphant T, Peterson P, et al., SciPy: Open Source Scientific Tools for Python, 2001. [Online; accessed 2017–09-20].

[67]. Neese F, Wiley Interdiscip. Rev. Comput. Mol. Sci 2012, 2, 73.
[68]. Petrenko T, Kossmann S, Neese F, J. Chem. Phys 2011, 134, 054116.

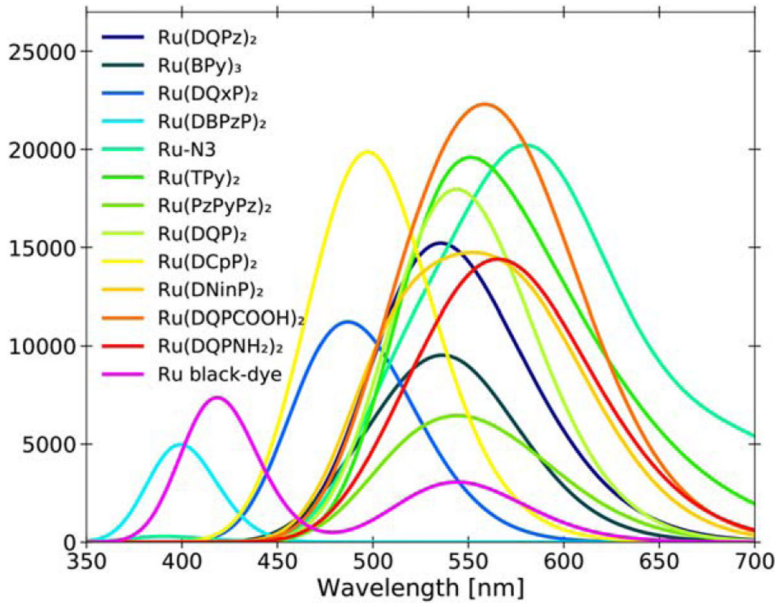

Figure 1.
Calculated PM6CI//PM6/Ru UV/vis spectra of the training set.

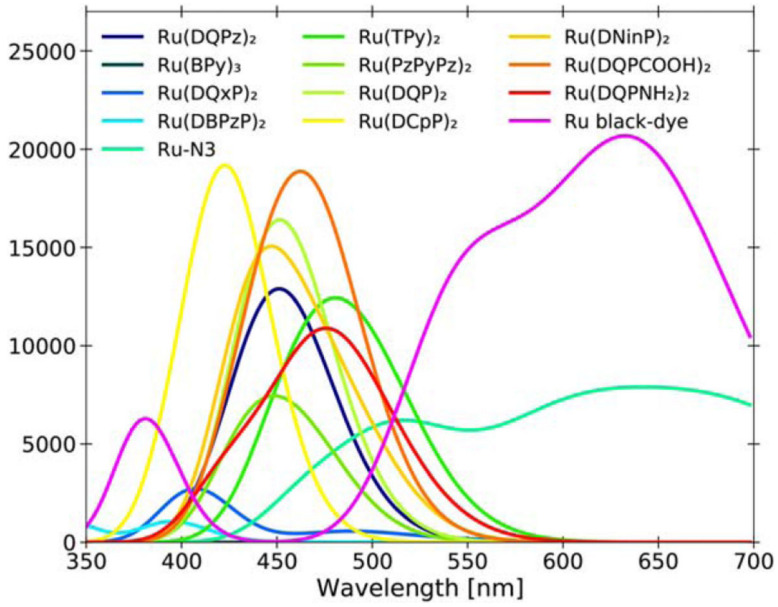

Figure 2.
Calculated PM6CI//PM6/rRu UV/vis spectra of the training set.

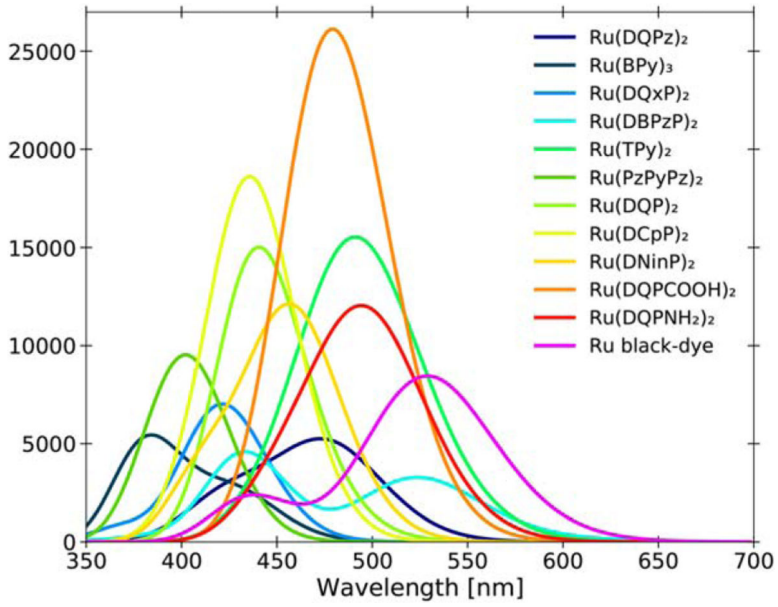

Figure 3.
Calculated PM6scCI//PM6/rRu UV/vis spectra of the training set.

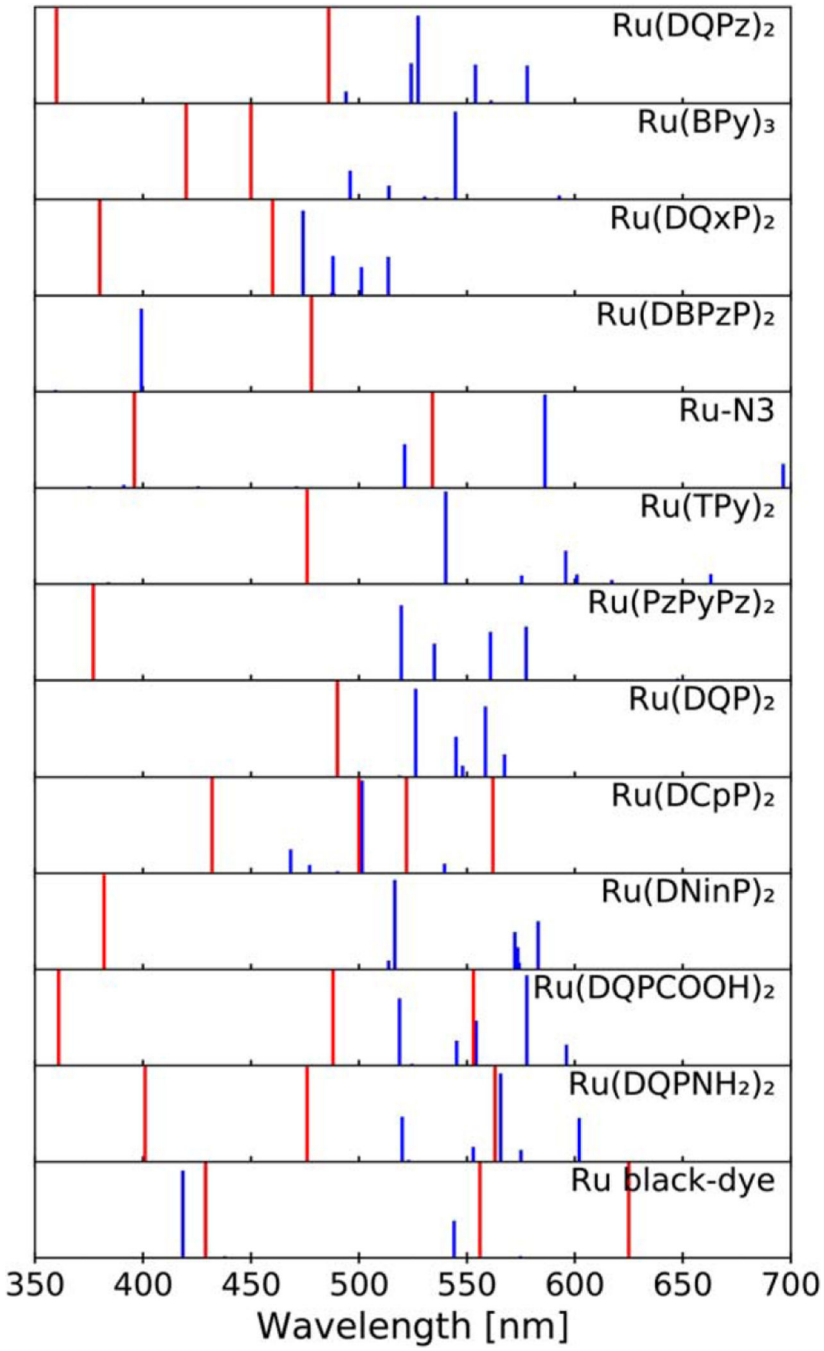

Figure 4.
Comparison of calculated PM6CI//PM6/Ru transitions (blue) and experimental maxima (red) of the training set.

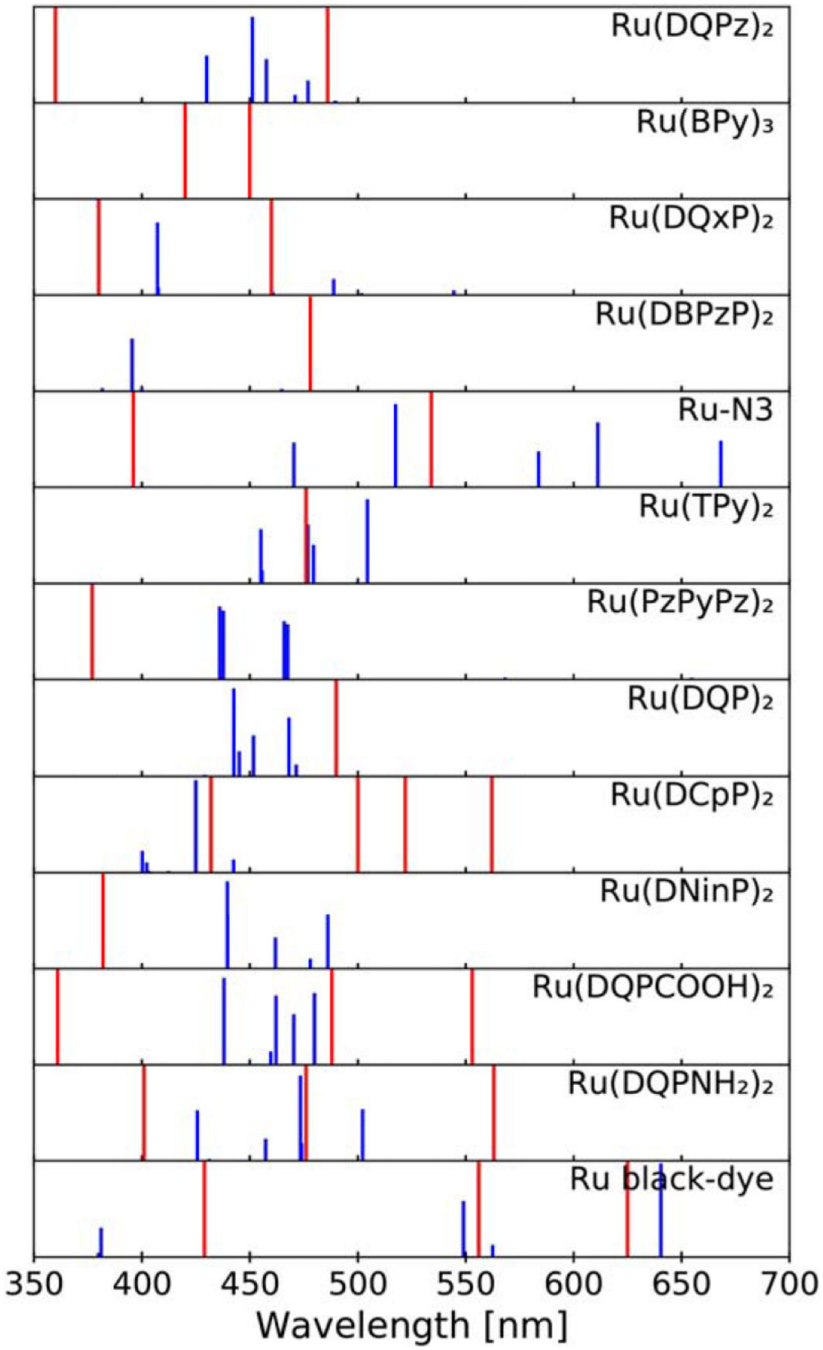

Figure 5.
Comparison of calculated PM6CI//PM6/rRu transitions (blue) and experimental maxima (red) of the training set.

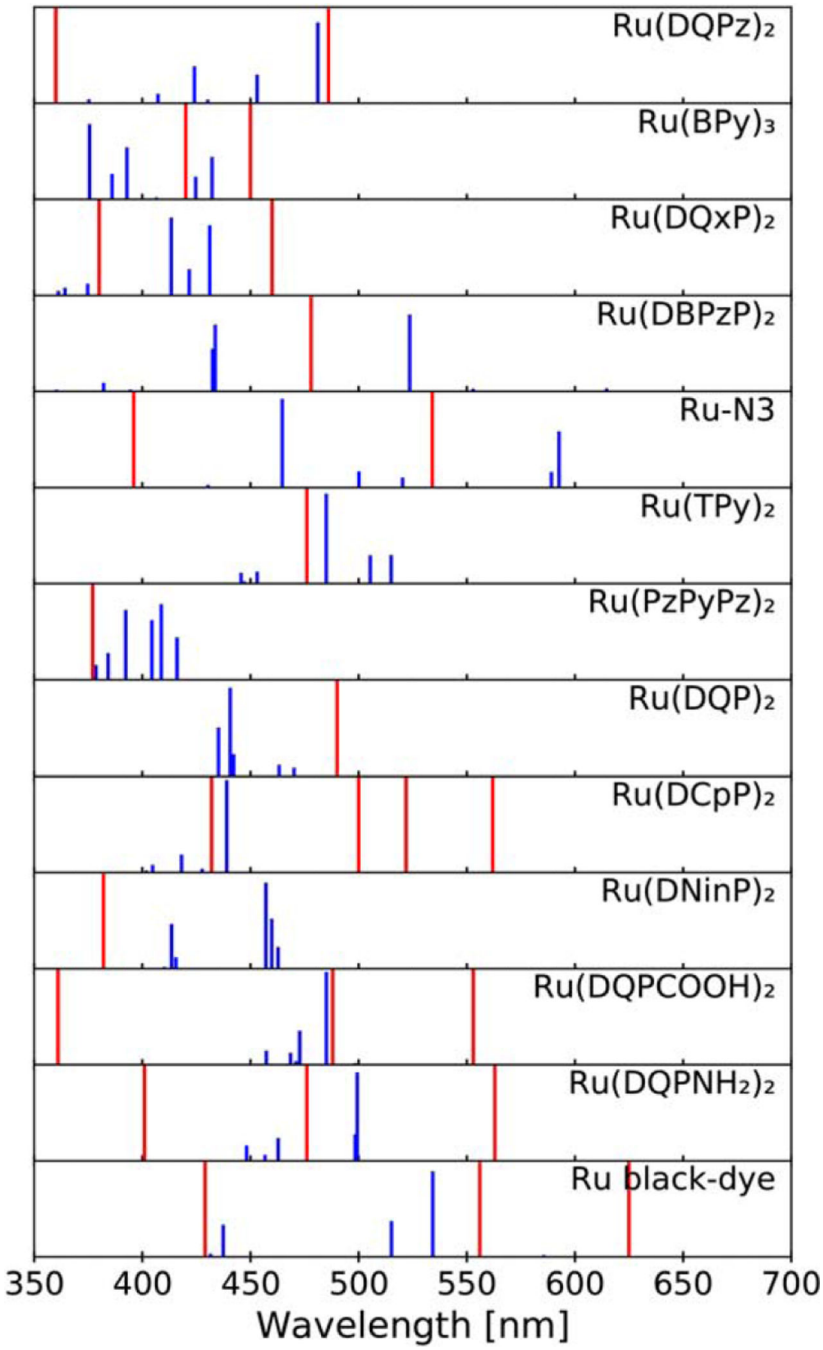

Figure 6.
Comparison of calculated PM6scCI//PM6/rRu transitions (blue) and experimental maxima (red) of the training set.

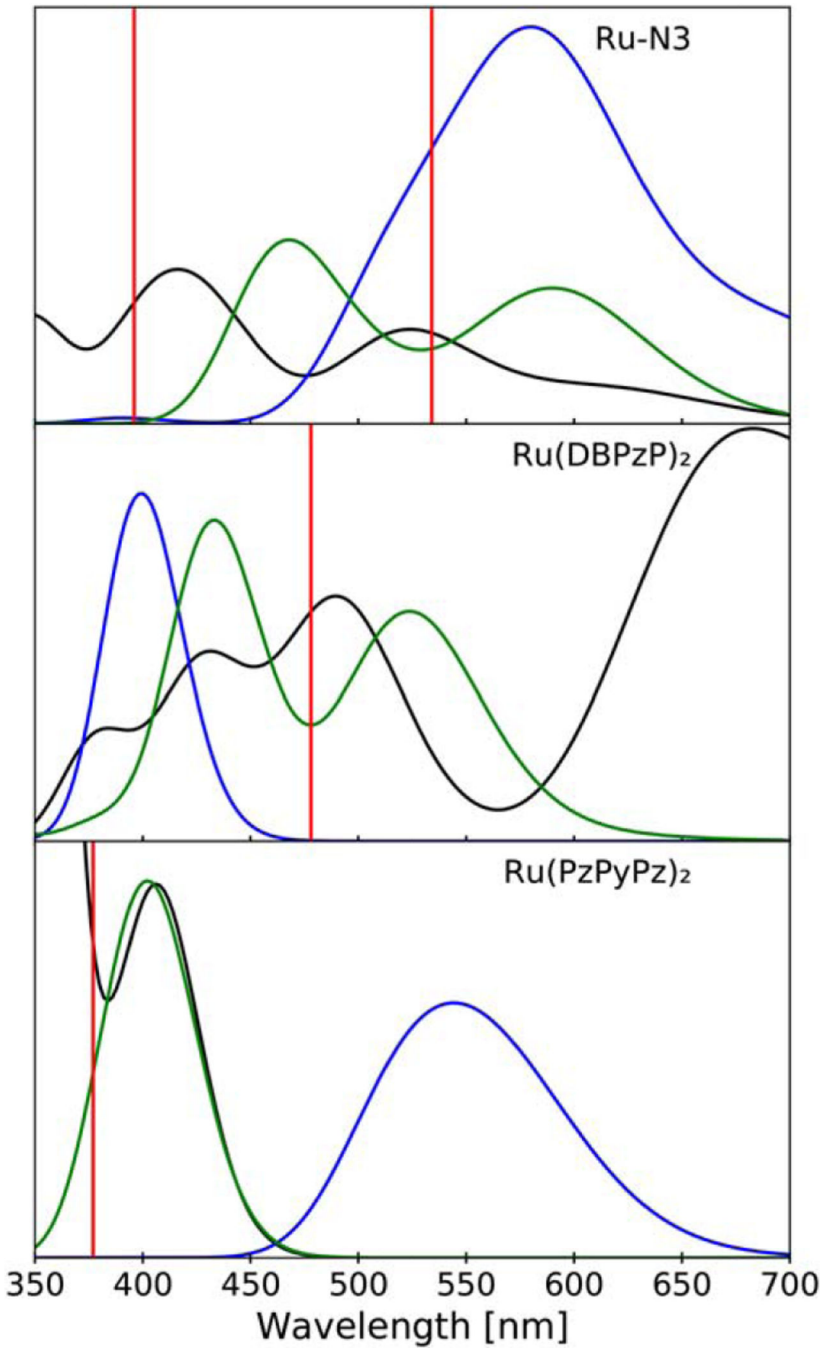

Figure 7.
Comparison of spectra between experimental maxima (red lines), TDDFT (black), PM6CI (blue), and PM6scCI (green) for the compounds indicated.

Table 1.

Absorption energies used in fitting the CI model.

Name	Compound	Absorption	energies [nm]
$Ru(BPy)_3$	$[Ru(BPy)_3]^{2+}$	450 420	
$Ru(TPy)_2$	$[Ru(TPy)_2]^{2+}$	476 310	
Ru-N3	$Ru[BPy—2COOH)_2(NCS)_2$	534 396	313
Ru black-dye	$[Ru(TPy—COOH)(NCS)_3]^{3-}$	625 556	429 344 330
$Ru(PzPyPz)_2$	$[Ru(PzPyPz)_2]^{2+}$	377	
$Ru(DQP)_2$	$[Ru(DQP)_2]^{2+}$	490 336	281
$Ru(DQPCOOH)_2$	$[Ru(DQPCOOH)_2]^{2+}$	553 488	361
$Ru(DQPNH_2)_2$	$[Ru(DQPNH_2)_2]^{2+}$	563 476	401 321
$Ru(DQPz)_2$	$[Ru(DQPz)_2]^{2+}$	486 360	344
$Ru(DBPzP)_2$	$[Ru(DBPzP)_2]^{2+}$	478 348	313
$Ru(DNinP)_2$	$[Ru(DNinP)_2]^{2+}$	382 310	
$Ru(DQxP)_2$	$[Ru(DQxP)_2]^{2+}$	460 380	340
$Ru(DCpP)_2$	$[Ru(DCpP)_2]^{2+}$	562 522	500 432 331

Table 2.

Optimized atomic parameter values for the PM6 basis set for Ru.

Parameter	Value	Parameter	Value
$U_{ss}[E_h]$	−44.90152100	G_{ss}	4.41364279
$U_{pp}[E_h]$	−41.42440900	G_{pp}	22.49044761
$U_{dd}[E_h]$	−37.93451400	G_{sp}	5.35699582
$\beta_s[E_h^{-1}]$	−12.85950800	H_{sp}	0.00805809
$\beta_p[E_h^{-1}]$	−8.47551800	Gp2	19.59995666
$\beta_d[E_h^{-1}]$	−3.83079700	F0sd	5.91740400
$\zeta_s[a_0^{-1}]$	1.45919500	G2sd	5.85973800
$\zeta_p[a_0^{-1}]$	5.53720100		
$\zeta_d[a_0^{-1}]$	2.09316400		
$z_{sn}[a_0^{-1}]$	0.98444900		
$z_{pn}[a_0^{-1}]$	4.58661300		
$z_{dn}[a_0^{-1}]$	0.76533200		

Table 3.

Optimized diatomic parameter values for the PM6 basis set for Ru.

Bond	$\alpha_{ij}\left[a_0^{-1}\right]$	x_{ij}
Ru–H	2.89201896	7.14609528
Ru–C	2.78870566	1.09168381
Ru–N	3.10082239	2.32425209

Table 4.

Values of optimized scaling parameters used in the semiempirical model.

Parameter	Value
f_{ss}	1.0097
f_{sp}	1.0182
f_{sd}	1.0009
f_{pp}	1.0082
f_{pd}	1.0090
f_{dd}	0.98443

Table 5.

Values of calculated absorption energies (nm) compared to experimental values used in fitting the semiempirical model. Common names for some compounds are given in italics.

	Spectral line		
Compound	**Calc**	**Expt**	**Error**
$[Ru(BPy)_3]^{2+}$	432.14	420	12.14
	424.57	420	4.57
	392.81	420	−27.19
	385.96	420	−34.05
	375.49	420	−44.51
$[Ru(TPy)_2]^{2+}$	514.97	476	38.97
	505.29	476	29.29
	484.94	476	8.94
	453.06	476	−22.94
	445.59	476	−30.42
$Ru(BPy\text{-}2COOH)_2(NCS)_2$	592.52	534	58.52
(Ru-N3)	589.00	534	55.00
	520.31	534	−13.69
	500.08	534	−33.92
	464.64	534	−69.36
	430.26	396	34.26
$[Ru(TPy\text{-}COOH)(NCS)_3]^{3-}$	534.16	556	−21.85
(*Ru black-dye*)	515.12	556	−40.89
	437.32	428	8.32
	431.44	428	2.45
$[Ru(PzPyPz)_2]^{2+}$	415.96	377	38.96
	408.73	377	31.73
	404.37	377	27.37
	392.24	377	15.24
	384.13	377	7.12
	378.50	377	1.50
$[Ru(DQP)_2]^{2+}$	470.14	489	−19.86
	463.20	489	−26.80
	442.14	489	−47.86
	440.52	489	−49.48
	435.14	489	−54.86
$[Ru(DQPCOOH)_2]^{2+}$	485.00	487	−3.00
	472.66	487	−15.33
	470.98	487	−17.02
	468.50	487	−19.49
	457.29	487	−30.71

	Spectral line		
Compound	**Calc**	**Expt**	**Error**
$[Ru(DQPNH_2)_2]^{2+}$	499.31	476	23.31
	498.33	476	22.33
	462.77	476	−13.24
	456.68	476	−19.32
	448.15	476	−27.86
$[Ru(DQPz)_2]^{2+}$	481.04	486	−4.96
	453.04	486	−32.96
	430.17	486	−55.83
	423.96	486	−62.04
	407.23	360	47.23
	375.16	360	15.16
$[Ru(DBPzP)_2]^{2+}$	523.58	478	45.58
	433.63	478	−44.37
	432.38	478	−45.62
	382.01	347	34.01
	305.30	312	−7.69
$[Ru(DNinP)_2]^{2+}$	462.73	381	80.74
	459.78	381	77.78
	457.12	381	75.12
	415.44	381	33.45
	413.50	381	31.51
$[Ru(DQxP)_2]^{2+}$	431.08	460	−28.92
	421.59	460	−38.42
	413.35	380	33.34
	374.63	380	−5.37
	364.15	380	-15.86
	361.08	380	−18.92
$[Ru(DCpP)_2]^{2+}$	438.93	432	6.93
	427.56	432	−4.44
	418.00	432	−14.00
	404.74	432	−27.26

Table 6.

Values (nm) of statistical measures of PM6 CI models. The mean unsigned and mean signed deviations (MUD, MSD), standard deviation (σ), minimum, and maximum of the error are given.

	PM6CI// PM6	**PM6CI// PM6/rRu**	**PM6scCI// PM6/rRu**
MSD	58.63	−41.24	−2.83
MUD	67.27	103.75	29.72
σ	72.57	58.81	19.20
Min	0.10	20.96	1.50
Max	327.21	311.77	80.74

Note that the PM6CI//PM6 calculation did not produce any singlet–singlet transitions in the range of 300–730 nm for $Ru(TPy)_2$, and the PM6CI//PM6/rRu calculation similarly skipped $Ru(BPy)_3$, so there are no contributions in the error statistics from those compounds.